Experimental Study of Thermal Bubble Pump

Dr. Safaa H. Faisal
Department of Mechanical Engineering
University of Basrah
College of Technical

Ass. Prof. Dr. Abdulwadood S. Shihab
Department of Mechanical Engineering
University of Basrah
College of Technical

Prof. Dr. Saleh E. Najim
Department of Mechanical Engineering
University of Basrah
College of Engineering

***Abstract*- In this study, a numerical investigation has been carried out for single phase flow behavior for thirty six internally finned tubes to demonstrate the effect of axial pitch to fin height ratio (p/e) for 0.8≤p/e≤6.345, helix angle of internal fins (β) for 30°≤β≤70°, apex angle of internal fins (α) for 0°≤α≤53.13°, internal fin height (e) for 0.6mm≤e≤1.0mm, internal tube diameter (di) with 14 mm and Reynolds number (Re) of single phase flow for 10000≤Re≤50000 on enhancement of forced convection heat transfer and reduction of friction factor by using ANSYS CFX program. It solves the three-dimensional Navier-Stokes equations for steady state turbulent with SST model and enhance wall treatment. The numerical analysis provided at fully developed velocity and temperature. Numerical results showed that the smallest axial pitch to fin height ratio (p/e) =0.8 and with apex angle α=10 degree provided enhancement of heat transfer of 2.8 to 3.55 times higher than of smooth tube. Finally, present numerical results are seen to be in good agreement with literature experimental correlations.**

Key words: Bubble pump, Vapor lift, Two-phase flow, Slug flow, vapor absorption refrigerator.

1. Introduction

The bubble pump is merely a vertical tube that does not contain any moving parts and is submerged at its lower part in a liquid to a certain level (see Fig. (1)). Heat is applied at the bottom of the tube (the vapor generator) at a rate sufficient to vaporize some of the liquid. The resulting vapor bubbles occupy completely the cross section of the tub and rises upward. The rising vapor bubbles acts like a piston and due to its buoyancy force it lifts a corresponding amount of liquid to the top of the bubble pump (the separator). The main application of vapor-lift pump is to replace the mechanical pump in absorption refrigeration system. This will leads to introduce a fully heat activated refrigeration system.

In the recent years, many researches have been carried out on VARS driven by bubble pumps. This will reduce the difficulties associated with the driving energy of the VARS. The absorption refrigeration system without a mechanical circulating device becomes more attractive, since this system is driven fully by the heat source.

Pfaff et al. [1] studied the bubble pump with a lithium bromide-water vapor absorption cycle. They developed a mathematical model using the manometer principle to evaluate the bubble pump performance. They found that the pumping ratio is independent of the heat input. However, the frequency of the pumping action increases as the heat inputs to the bubble pump increases, or if the tube diameter decreases.

Delano (1998) [2] studied theoretically and experimentally the vapor bubble pump used in the Einstein diffusion Vapor Absorption Refrigeration System (BPVARS). The theoretical results were correlated to fit the experimental date. It was shown that an increase in the tube diameter would decrease the friction factor and therefore resulting an increase in the flow rate through the bubble pump.

Sathe (2001) [3], studied theoretically and experimentally the vapor-lift pump that used for the diffusion BPVARS. He used methyl alcohol (methanol) as a tested fluid. He found that the frequency of pumping action (fluid pulses out of the bubble pump per unit time) increases with increase in the heat input.

Koyfman et al. (2003) [4], carried out an experimental investigation on a closed continuous bubble pump apparatus using organic solvent as absorbent and hydro-chlorofluorocarbon (R22) as a refrigerant. The results showed that the motive head is one of the most dominant parameters influencing the bubble pump performance.

Zhang et al (2006) [5], carried out an experimental investigations on the performance of the bubble pump with a lunate channel using Lithium Bromide as absorbent and water as refrigerant. They claimed that this configuration will enhance the performance of the bubble pump. They concluded that a pump with combined diameters ratio of 16/32 mm. is suitable for a refrigerator with cooling capacity of 4.8 kW using heat source temperature of $75^{o}C$.

Vicatos and Bennett (2007) [6], proposed multi tube bubble pump for enhancing the performance of the diffusion BPVARS. The Delano's model (1998) was modified to evaluate the performance of multi tube bubble pump arrangement. It is concluded that the multiple lift tube bubble pump is a viable and workable solution to increase the refrigeration capacity without any change in the coefficient of performance.

Shihab and Morad (2012) [7] conducted an experimental test to study the pumping characteristics of a vapor-bubble pump based on water properties. Depending on the obtained experimental data, they reconstruct and correct the theoretical mathematical model of the bubble pump to fit their experimental results.

Faisal (2012) [8], suggested a new theoretical analysis as an approach for modeling the performance of thermal bubble pump. Results indicate that the maximum pumping capacity is positively increased with increasing the submergence ratio and tube diameter at a fixed riser tube length. The maximum pumping capacity is found to be independent of the liquid temperature at the inlet to the generator under the assumption of stable operation of the pump. It is obtained that the slip ratio decreases with the increasing of the submergence ratio and slightly decrease with the decreasing of the tube diameter.

The aim of the present experimental work of the vapor bubble pump is to examine the actual performance of the vapor bubble pump at various geometrical configurations. This will help to validate any bubble pump mathematical model based on the water properties. The valid model then can be safely applied with any other fluids or mixture properties.

2. Theoretical Background

In order to predict the pumping capacity for a specified pump configuration and operation parameters, the analytical model

should base on the mass, momentum, and the energy conservation.

Referring to the fig. (1), applying the mass balance equation from point 1 to point 2 yields [8]

$$\dot{m}_{tot} = \dot{m}_L + \dot{m}_v \quad (1)$$

Appling Bernoulli equation from the liquid surface at the downcomer to point 1 yields [8]:

$$P_1 = P_{atm} + \rho_0 g(R_{subm} L_{ris} + Z_{gen}) - 0.5\rho_1 U_1^2 \quad (2)$$

At the generator, heat energy is added to produce mixture of vapor and liquid. Applying the energy balance for the generator gives [8]:

$$Q_{gen} = \dot{m}_{tot}(h_2 - h_1) \quad (3)$$

Next, applying the conservation of momentum for the generator results in [8]:

$$\dot{m}_{tot}(U_2 - U_1) = P_1 A_{gen} - P_2 A_{gen} - \rho_h A_{gen} Z_{gen} g - f(0.5\rho U_2^2) Z_{gen} \pi D_{gen} \quad (4)$$

Actually, the most important challenge for any model is to represent an expression to calculate the two-phase pressure drop across the riser tube. Determining such expression, the analytical model of the bubble pump will be completed. This can be achieved through expressing the pressure drop to become as the ability of the buoyancy force to overcome the gravitational and friction force of the flowing mixture [8]

$$(P_2 - P_{atm}) = \Delta P_{TP} = \Delta P_{gra} + \Delta P_{fri} \quad (5)$$

The gravitation term represents the weight of the fluids (body force) and the friction term represents the shear force (surface force) at the wall.

3. Experimental Work

A non-continuous experimental system was designed, built and successfully operated. The experimental rig was built in a way that allows easily change in geometry of the system. The experiments were performed in which some of the parameters affecting the bubble pump performance (tube diameters and submergence ratios), were changed. A view of the experimental rig is shown in the fig. (2). The schematic diagram of the experimental setup is shown in the fig. (3) and the dimensions of the main components are shown in the fig.(4).

4. Rig's Components

The test rig comprises of the following components and instruments.

A- The Tube Riser: It is the main part of the bubble pump, which connect the vapor generator at its base and the liquid-vapor separator at the top. The tested tubes are selected of glass to allow the observation of the flow pattern. The observation section is located at the tube mid-point. Sample images of the two phase regime are shown in fig.(5).

B- The Liquid-Vapor Separator: It is made of a copper tube and comprises a sight glass at its front side where the riser top end can be viewed to watch the pumping action. This separator is fabricated together with the condenser as a one piece and supplied with four baffles, one vertical and three horizontal, to ensure no liquid drops companying the vapor in its way to the condenser. Its dimensions are shown in the fig. (-4- A).

C- The Condenser: It is made of copper tubes and fabricated as a shell and tube heat exchanger. The vapor flows inside the annulus while cooling water flows inside the inner tube. Its dimensions are shown in the fig. (-4- B).

D- The Over Flow Assembly: This assembly is responsible for adjusting a constant and stable water level at the riser tube. It consists of the following component:

(i)-Over Flow Water Receiver: It is of 20 L capacity and made of iron sheets. It receives hot water from both the over flow pipe and from the separator (pumped liquid).

(ii)- Over Flow Pipe: It is merely a piece of copper tube, which is connected to the down comer pipe and to the over flow water receiver using flexible tubes so that its level can be adjusted as required to regulate the requested submergence ratio. The flooded liquid out of it is moved back to the water receiver. Its dimensions are shown in the fig. (-4- C).

(iii)- Circulating Pump: This pump is of 30 L/min that is used to circulate the hot water between the downcomer pipe and the over flow water reservoir.

E- The Downcomer Receiver: It is a copper tube of 5.1cm diameter and 1.9m long. A heating element of (1500 W) is placed in at the bottom of this pipe to adjust and stabilize the generator inlet temperature.

F- The Generator: It is made of a copper pipe, inside which a heating element of (1500 W) is placed. Its dimensions are shown in fig.(-4- D).

G- The Water Cooler: This cooler is used to supply the chilled water to the condenser via a circulating pump of 30 L/min capacity .

H- The Insulations: To reduce the heat losses, the entire setup was fully insulated by 0.5 cm thickness of asbestos and then by two layers of glass wool each of 2.45cm thickness.

I- The Holding Truss: To facilitate the mounting of the components, a truss that made of perforated L-section iron channels is used.

5. Measuring Instruments

The test rig comprises of the following instruments:

A- Variac: It is used for controlling the power input to the heating element that placed in the generator. Its specifications are: maximum current 8A, regulated voltage range 0-220V with resolution of 0.5V.

B- Digital Multi-meters: It is used to measure the heating power input to the generator in term of volts and amperes. The milli-voltmeter is used to measure the output from the thermocouples. Their specifications are:

(i)-The milli-voltmeter: It is made by Thurlby electronics Ltd, model 1503 digital type. The maximum reading is 32mV with 0.01 mV resolution. Its accuracy is 0.005 mV.

(ii)-The Voltmeter: It is made by KONSTAR Electronics model DT-266. The maximum reading is 600V, resolution is 1V, and accuracy is 0.5 V.

(iii)- The Ammeter: It is made by Digital Technology Ltd. model DT9205A. The resolution is 0.1A with maximum reading of 20A. Its accuracy is 0.05 A.

C- Thermocouple Wires: These wires (of K-type) are spot welded and carefully inserted into the main flow stream at four locations in the experimental rig, (see fig. (2)). Calibration is done against mercury thermometer.

D- The Balances: Two balances are Calibrated against standard weight and used: :

(i)- The balance used for measuring the pumped water flow rate. It is made by DIUJIANG Co., maximum reading 30kg with resolution of 1g. Its accuracy is 0.5g.

(ii)- The balance used for measuring the condensed vapor. It is made by DENVER Instruments Inc. the maximum reading is 200g with resolution of 0.01g. Its accuracy is 0.005g.

E- Stop Watches: To measure the time of collection the pumped water and condensed vapor, two stop watches are used. It is made by G.U.N.T GmbH each of resolution 0.01 sec. Its accuracy is 0.005 s.

6. Rig Construction and Operation

The experimental rig consists of three main loops. The first loop is for the chilled water necessary for condensing the vapor. The second loop is for the pumped water out of the bubble pump that returns to the main hot water receiver. The third loop is for the over flow water recirculation that necessary for fixing the driving head during the test.

The generator is joined to the bottom of the downcomer tube by a short piece of copper tube of 1.27cm diameter in order to form a U-shape. A drain valve is used to empty the rig for preparing it to the next test. The test tube is attached to the generator exit using a high temperature resistance rubber piece. The upper end of the test tube is attached to the separator-condenser assembly. The join between the tube riser and the separator-condenser assembly is treated using a high temperature rubber maker. This glue is easy to remove in case of replacing the tube or the generator.

The chilled water is circulated through the condenser using flexible tubes of 1.27cm diameter while the pumped liquid is drained back to the hot water receiver via a flexible tube of 2.5cm diameter. The overflow pipe is connected to the downcomer via flexible tubes of 2.5cm diameter. The drain from the overflow pipe is directed back to the main hot water receiver. A level indicator is attached to the downcomer pipe. The hot water circulating pump is connected to the main hot water receiver and the downcomer pipe using reinforced flexible tubes. These flexible tubes resist the deformation caused by the high temperature. The visual observation of the flow regime was made through a section of about 15cm located at the midpoint in the tested riser tube.

7. Test Procedure

For a given tube diameter and submergence ratio, the test is done as following:

1- Firstly, the system is filled with a pure water.
2- The two heating elements located at the downcomer pipe and the generator is powered on with a full load in order to hurrying up the warming of the rig. During this process the vapor vent valve, located at the top of the separator, is opened and the circulating pump for the cooling water is off. This situation will save the iced cooling water until the steady state is reached. No records were done during the warming process and the unsteady operation of the bubble pump can be easily observed. The steady state operation is noted by examining the temperature measurement variation round the rig besides the observation of the two phase flow in the riser tube.
3- When the steady state operation is reached, the vapor vent valve is closed, cooling water pump in turned on, and the heat input to the generator is controlled via the variac.
4- Measurement started after five minutes by collecting masses of pumped water and condensate vapor for a given period of time. This process requires 10-15 minutes according to the amount of input heat. Each reading in repeated three times to reduce the error.
5- After the run completes, the generator heat input is varied and the measurements started again. The whole test campaign began with higher input power and gradually decreased. The complete test of a single submergence ratio requires 3-4hr.

8. Test Records

The mass flow rates of the pumped water and condensed vapor are calculated as:

$$\dot{m}_L = \frac{Collected\ mass}{Time\ of\ collection}\ (kg/s) \quad (6)$$

$$\dot{m}_v = \frac{Collected\ mass/1000}{Time\ of\ collection}\ (kg/s) \quad (7)$$

The heating power input to the generator is calculated as:

$$Q_{gen} = Ampers * Volts * 0.8\ \ (W) \quad (8)$$

The value 0.8 is the power factor recommended for heating elements.

The milli volts output from the thermocouples is converted to a temperature measurement via the calibrations equation as:

$$T = milliVolts * 24.4416 + T_{amb} \quad (9)$$

9. Results and discussion

The experimental behavior assessments of the bubble pump is done using three tubes diameters 6.5, 10, and 14 mm while the riser tube length is fixed to 1.5 m. The selected submergence ratios, R_{subm}, are 0.5, 0.6, 0.7, and 0.8. The heating power range depends on the riser tube diameter as follows:

20-200 W (for the 6.5mm tube).
100-1000 W (for the 10mm tube).
100-1300 W (for the 14mm tube).

A preliminary rig design helps to stabilize the input temperature around 100°C. Then the rig is redesigned so that the input temperature could be stabilized around 102°C. The preliminary design is used to test only the 10mm riser tube while the modified rig design is used to test all the selected riser tube diameters.

9-1 Two-Phase Flow Observation:

The two-phase flow regime plays an important role in the operation of the bubble pump. Fig.(5) shows typical two phase observations for four main two phase regims.
It is observed that for the small tube diameter 6.5mm, the intermittent slug flow cover mostly all the operating range of the bubble pump with different amount of heat supply. Although the churn and annular may appear at the higher heat input but the bubbly flow was not o bserved even at low heat input. At low heat input, the produced dispersed bubbles have no chance to penetrate up ward through narrow water blocked tube and so they merge with each other's to form what is called "Taylor bubbles". This fact is confirmed by the observed pulsing behavior via the sight glass at the riser pipe exit.
For the larger tube diameters of 10 and 14 mm, it is observed that at low heat input, the bubbly flow could be easily observed. This regime could not cause any pumping with low submergence ratios. The bubbles can make an upward way through water and burst at the free surface causing some disturbance in the water level in the tube riser. The gradual increase in the submergence ratio outcomes higher fluctuation of water level below the exit point without any discharge. With higher values of the submergence ratios (at some threshold point of pumping depending on the tube diameter), the bubbly flow could cause a pumping action. The physical explanation is that the average density due to the bubbly regime is just able to balance a low lift head and starts few liquid pumping.
An intermitting pumping operation of the bubble pump was also observed when the heat input is gradually increased. At an intermediate generator heat supply and low input liquid temperature, the liquid is still subcooled with some nuclear boiling at the generator, so the water becomes oscillate within the riser column. During this time, with more heat supply, more vapor is produced pushing up the liquid indicating the threshold pumping point. In some times, more extra liquid could be pumped due to the effect of the high surface temperature of the generator and the heating element. During the pumping mode with continuous increasing of the heat supply , all the flow regimes can be recognized. The pumping starts with raising a single dancing cap type bubble followed by many medium sized bubbles. At some times, some medium sized bubbles could find a chance to merge forming larger Taylor bubbles (slug regime appears). These big bubbles appear suddenly causing big intermittent pulses at the riser exit. Next, the high-speed flow due to high vapor generation causes the long bubble to break down and form churn and then annular flow.
It is observed that larger tube diameters are more sensitive to the change in the input temperature. Generally, it is also observed that for a certain generator input temperature, there exists a minimum generator heat input that can cause the pumping startup (threshold point). The amount of this threshold heat is changed according to the diameter and the submergence ratios. Increasing the tube diameter will increase the threshold power while increasing the submergence ratio decreases the threshold power.

9-2 The Pumping Capacity:

Figs. 6, (a, b, c and d) show the comparison between the present experimental and the theoretical pumping capacity [8] with input temperature 100 °C (done by preliminary rig design). These Fig. s indicate that the experimental results have a comparable trend in their variation with that predicted by the theoretical model. All testes showed that there exists a maximum pumping liquid at some generator heat input for each submergence ratio. This experimental manner verified the applicability of the theoretical model proposed by [8] to describe the bubble pump behavior. However, it can be seen that the theoretical model could predict only the maximum pumping capacity. At other operational point, the model may fail to predict the discharge behaviors apart from the peak point due to changing the flow regime far from the slug flow. Generally, the difference between the experimental and the theoretical pumping capacity is quite understood since the analytical model involves several assumptions that are difficult to be attained experimentally. The departure of the predicted theoretical maximum pumping capacity are 5.2% , 5%, 8.2%, and 11.6% for the four selected submergence ratios 0.5, 0.6, 0.7, and 0.8 respectively.
Figs. 7 (a, b, c, and d) show the experimental pumping capacity for the small tested diameter of 6.5mm and using generator input temperature of 102°C. The Fig. s reveal that curve trend is the same as that discussed earilier but with smaller power required for threshold point and that required for maximum pumping capacity with some reduction of pumping capacity.
Figs. 8, (a, b, c, and d) show the experimental pumping capacity for the tested diameter of 10mm.
Examining the figs. (6) and (8), it tell an important remark about the location of the maximum pumping capacity. The location of the maximum point is directly affected by the generator input temperature, (as quite explained in [8]). Higher input temperature shifts the curve's peek point to the left and this makes the maximum pumping capacity to be easily observed at a low generator heat input. The problem is that for a small lowering in the input temperature results in a higher shifting of the maximum pumping capacity to a higher generator input heat. This value of shifted heat energy increases dramatically for the higher submergence ratios and riser tube diameters. Actually, this represents serious challenge for the experimental measurement of the maximum pumping capacity location, since any small fluctuation in input temperature or any heat losses will correspond to higher error in the maximum pumping capacity location.

It is worth noting that the experimental pumping capacity is affected by the separator pressure. So, the increase in separator pressure due to high flow rate of both the liquid and the vapor prevent the separator from stabilizing its pressure near the atmospheric as assumed. This fact is observed experimentally when the vent valve, up the separator is opened to reject the vapor to the atmosphere while the pump is still in operation. The result is an increase in the pumping capacity roughly by 4-6 % depending on the pump configuration.

Comparing the experimental results of the pumping capacity shown in figs. 8 (a, b, c, and d) with that already discussed in the figs. 6 (a, b, c, and d) confirm the fact that the generator inlet temperature has insignificant effect on the maximum pumping capacity. For the selected submergence ratios 0.5, 0.6, 0.7, and 0.8, the experimental maximum pumping capacity have changed by 1.7, 3.2, 3.2, and 1.3% as the input temperature increases from 100 to 102°C.

Figs. 9,(a, b, c, and d) show the experimental pumping capacity for the tested diameter of 14mm. Actually, all the remarks noted in the 10mm tested diameter is also noted for the 14mm tested diameter, but the maximum liquid discharge increases with increasing diameter with higher heat supply.

Fig. (10) shows comparison of the obtained experimental maximum pumping discharge with that of [7]. All curves show clearly that the maximum pumping capacity increase linearly as the submergence ratio increases.

The maximum experimental pumping capacities were fitted using linear approximation for the selected three riser tubes and the following correlations are obtained:

For $D_{ris}=6.5mm$:

$$\dot{m}_{L,max}=3.51*10^{-4}+22.74*10^{-3}\cdot R_{subm}$$

For $D_{ris}=10mm$:

$$\dot{m}_{L,max}=0.003622+0.06683\cdot R_{subm}$$

For $D_{ris}=10mm$:

$$\dot{m}_{L,max}=0.00175+0.135\cdot R_{subm}$$

9-3 The Vapor Mass Flow Rate:

Concerning the vapor flow rate, the figs. (11,12 and 13) demonstrate the experimental measurements of the vapor flow rates for the tested riser tubes. The Fig. s demonstrate that the vapour mass flow rate is nearly linear with input heat power. That is mainly due to introducing the liquid near the saturated state at the generator pressure. This will make the vapor mass flow rate and the input heat power linearly related with factor equal to the latent heat of evaporation

9-4 The Problems of Operation:

In order to share the experience with design and operation of such systems, the following problems are referred:

1. The leakage problems: These problems could occur in joints between the copper tubes and both the flexible tubes and the glass tubes. This problem can be overcome by increasing the used clamps. Besides, the applying the rubber maker silicon glue will ensure good adhering. This glue is characterized with high temperature resistance. For the riser glass tube, the rubber piece was very useful for mounting. It gives the pipes the required flexibility. The rigid fixing increase the risk of tube breaking.

2. The circulating of the cooling water back to the same cooler receiver causes the problem of the gradual increase in cooling water temperature. This situation could affect the condenser performance and more vapor will accumulate inside the generator without condensation. To solve this problem, a lot of ice is always kept standby so that the cooling water temperature will stabilize around 8°C. Furthermore, the spraying of the incoming water on the reservoir's wall (where the evaporator coil is located beneath) will minimize this problem.

3. The 8A variac suffer from the high temperature, due to the high current, which could damage the electric wires. This problem was solved by removing the case and mounting a cooling fan.

4. The hot water circulating pump suffers a high temperature that could damage the electric wires. To solve this problem this pump is modified by making it externally driven by electric motor via transmitting belt.

5. In the preliminary rig design, the over flow pipe was connected to the bottom of the downcomer pipe where a heating element is placed. By this configuration, it was believed that saturated water could be supplied to the generator. Actually, it is found that this arrangement could stabilize the temperature at the generator inlet to 100±0.5°C. So, in order to increase the input temperature above, it is necessary to move the connection point between the downcomer pipe and the overflow up to 60cm from the bottom of the downcomer pipe. The new configuration helps to stabilize the input temperature to 102±0.5°C. However, limited submergence ratios could be tested by the new configuration (above 0.4). This modification is necessary also to minimize the flashing occurred for the saturated water as it rise from the bottom of the downcomer pipe to the over flow pipe.

10. Conclusions

From the discussed results, the following conclusions are drawn:

1. The thermal bubble pump of a given diameter, submergence ratio, and length has a limited maximum pumping capacity at a specified vapor mass flow rate.

2. The maximum pumping capacity of the thermal bubble pump is found to be independent of the liquid temperature at the inlet to the generator, while it is positively affected when both the submergence ratio and riser tube diameter are increased.

3. From the two phase flow observation, it was observed that for the small tube diameter (6.5mm diameter), the intermittent slug flow cover mostly all the operating range of the bubble pump with different amount of heat supply. Besides, bubbly flow was not observed even at low heat input.

4. From the two phase flow observation, it was noted that for the larger tube diameters of 10 and 14 mm, and at low heat input, the bubbly flow could cause a pumping action with higher values of the submergence ratios (at some threshold point of pumping depending on the tube diameter).

5. The resulted vapour mass flow rate for the bubble pump is linearly related to the input power.

11. Recommendations

The experimental results obtained in this paper for the thermal bubble pump can led the way to implement full simulation for the bubble pump operated vapor absorption refrigeration system.

12. Nomenclatures

A:Area(m^2).
D: Diameter (m).
g: Gravity(m/s^2)
f: Friction factor.
h: Enthalpy(kJ/kg).
L: Length (m).
$\dot{m}$: Mass flow rate(kg/s).
P: Pressure (Pa)
Q: Heat power (W).
R_{subm}: Submergence ratio (-): It is the ratio of initial water level to the length of riser tube $= Z_d / L_{ris}$.
T: Temperature(°C).
U: Velocity(m/s).
Z: Height(m).
Z_d: Driving head(m).

***Greek Symbols*:**
ρ: Density (kg/m^3).
Δ: Difference

Subscripts
0,1,2**:** State point numbers.
*atm***:** Atmospheric**.**
gen: Generator
*gra***:** Gravitational**.**
*L***:** Liquid**.**
*ris***:** Riser tube**.**
*tot***:** Total**.**
*v***:** Vapor**.**

Abbreviations:
VARS:vapor absorption refrigeration system.
BPVARS: Bubble pump vapor absorption refrigeration system

13. References

[1]- Pfaff, M. , Sasavanan, R., Maiya, M.P. and Murthy, S.S., *"Studies on bubble pump for a water-lithium bromide vapour absorption refrigerator"*, Int. J. Refrigeration, Vol.21, NO.6, pp.452-562, 1998.
[2]- Delano, A.D, "Design Analysis of the Einstein Refrigeration Cycle", PhD Dissertation, Georgia Institute of Technology, Georgia, U.S.A, 1998.
[3]- Sathe, A.,"Experimental and Theoretical Studies on a Bubble Pump for a Diffusion Absorption Refrigeration System", M.Sc thesis, Indian Institute of Technology, Madras, 2001.
[4]- Koyfman, A., Jelinek, M., Levy, A. & Borde, I., "*An Experimental Investigation of Bubble Pump Performance For Diffusion Absorption Refrigeration System With Organic Working Fluids*", Applied Thermal Engineering, Vol.23, pp.1881-1894, 2003.
[5]- Zhang, L., Wua, Y. , Zheng, H. , Guoa, J. , & Chena, D. ,"*An Experimental Investigation on Performance of Bubble Pump with Lunate Channel for Absorption Refrigeration System*", Int.J.of Refrigeration, Vol.29, pp.815–822, 2006.
[6]- Vicatos, G., & Bennett, A., "*Multiple Lift Tube Pumps Boost Refrigeration Capacity in Absorption Plants*", Journal of Energy in South Africa, Vol.18, No.3,pp.49-57., 2007.
[7]-Shihab, A.W.S, Morad, A.M.A, *"Experimental Investigation of Water Vapor-Bubble Pump Characteristics and its Mathematical Model Reconstruction*", Engineering & Technology Journal, Vol. 30, No.11,pp.1870-1885. ,2012.
[8]- Faisal, S.H, " Performance Study of LiBr-Water Pumpless Absorption Refrigeration System", PhD Dissertation, University of Basah, Basrah , Iraq, 2012.

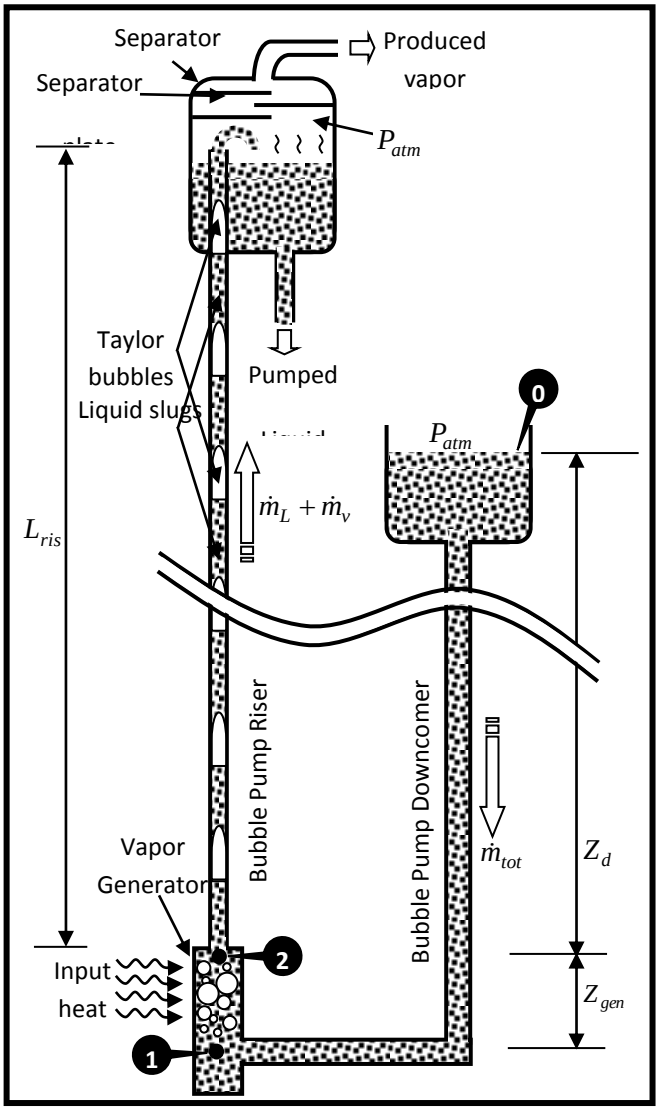

Fig.1 Schematic of the water-based thermal bubble pump.

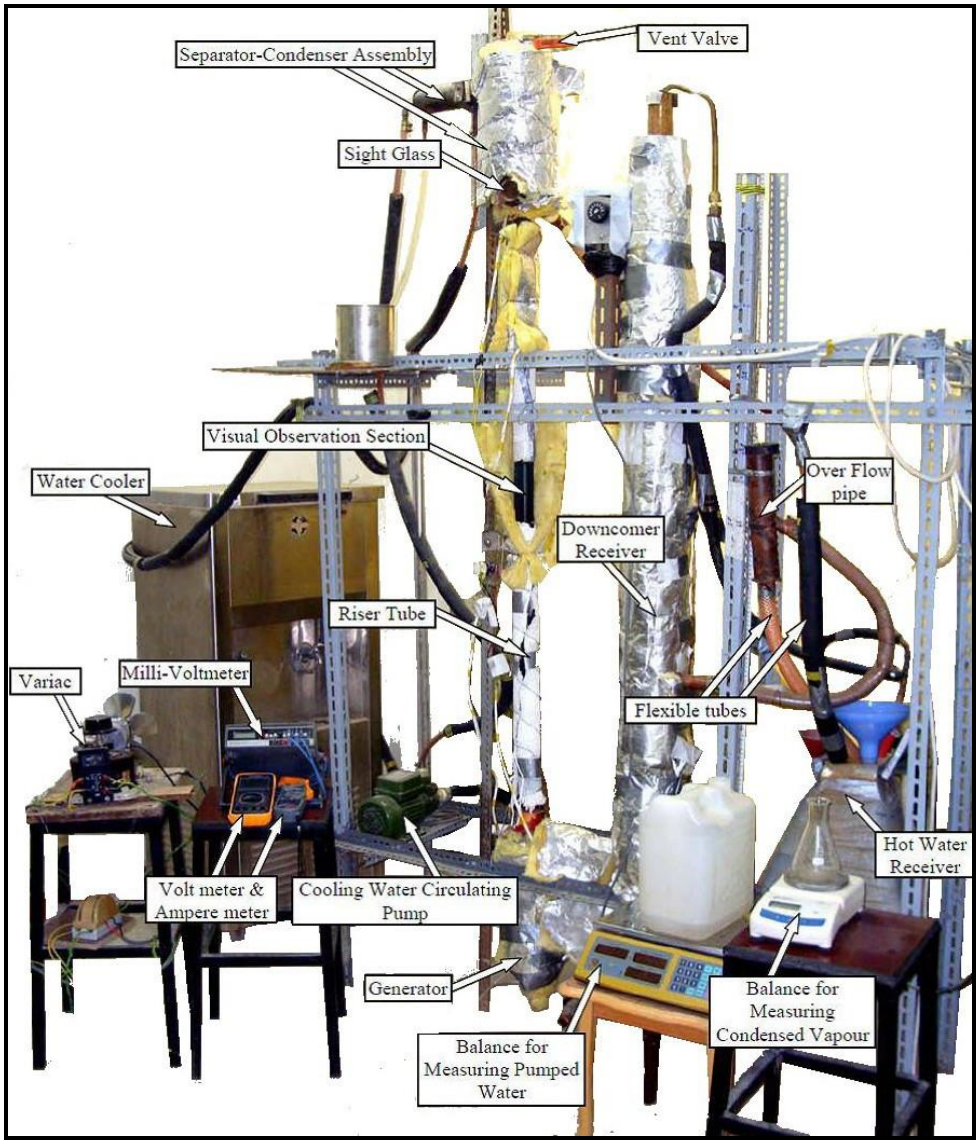

Fig. 2 Photo for the test rig.

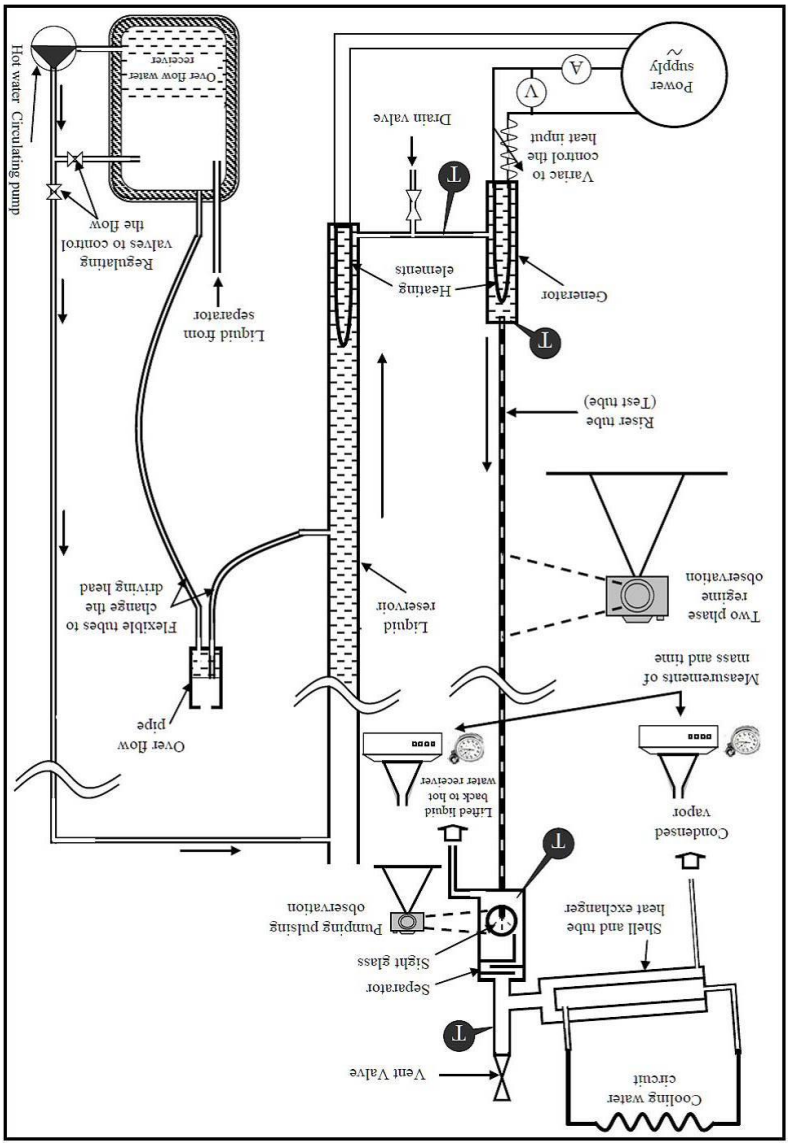

Fig. 3 Schematic diagram for the experimental setup

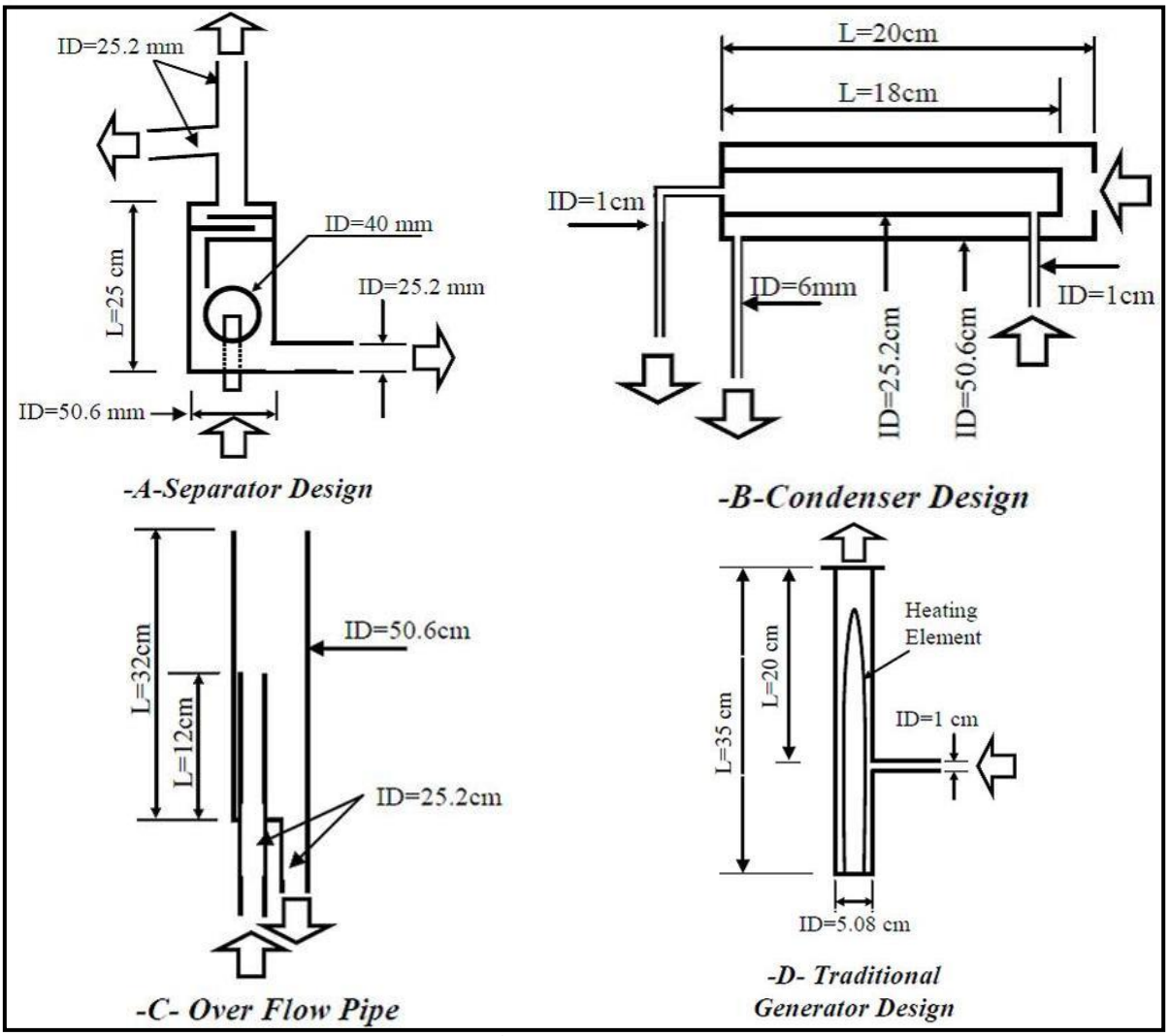

Fig. 4 The Dimensions of the main components making up the test rig.

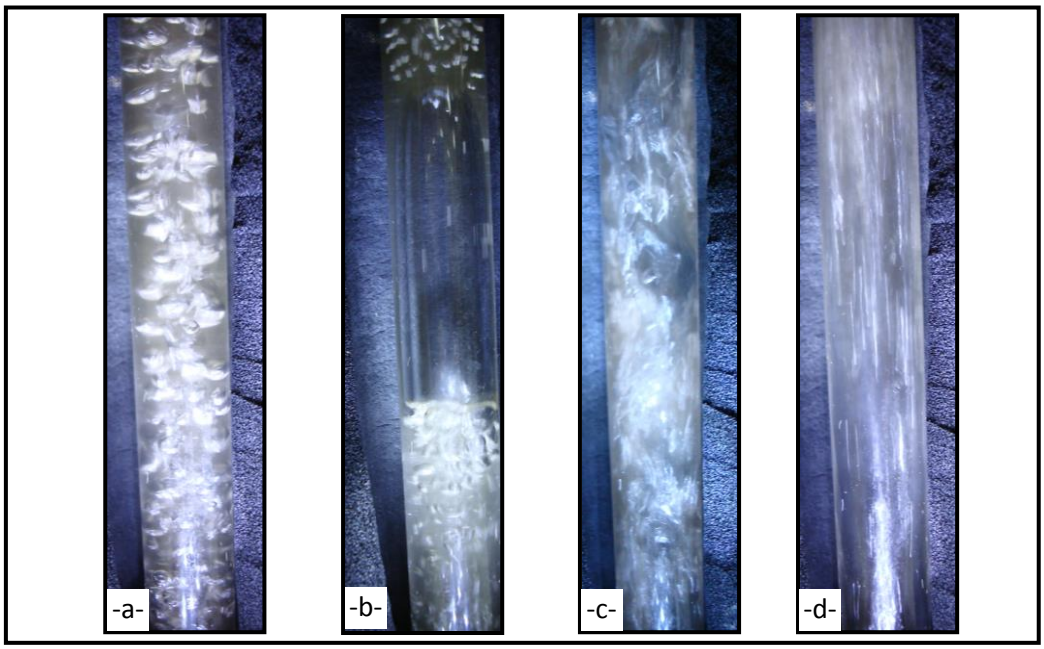

Fig.5 photos for the two phase flow regimes recognized through the observation section (-a- Bubbly, -b- Slug , -c- Churn, -d- Annular).

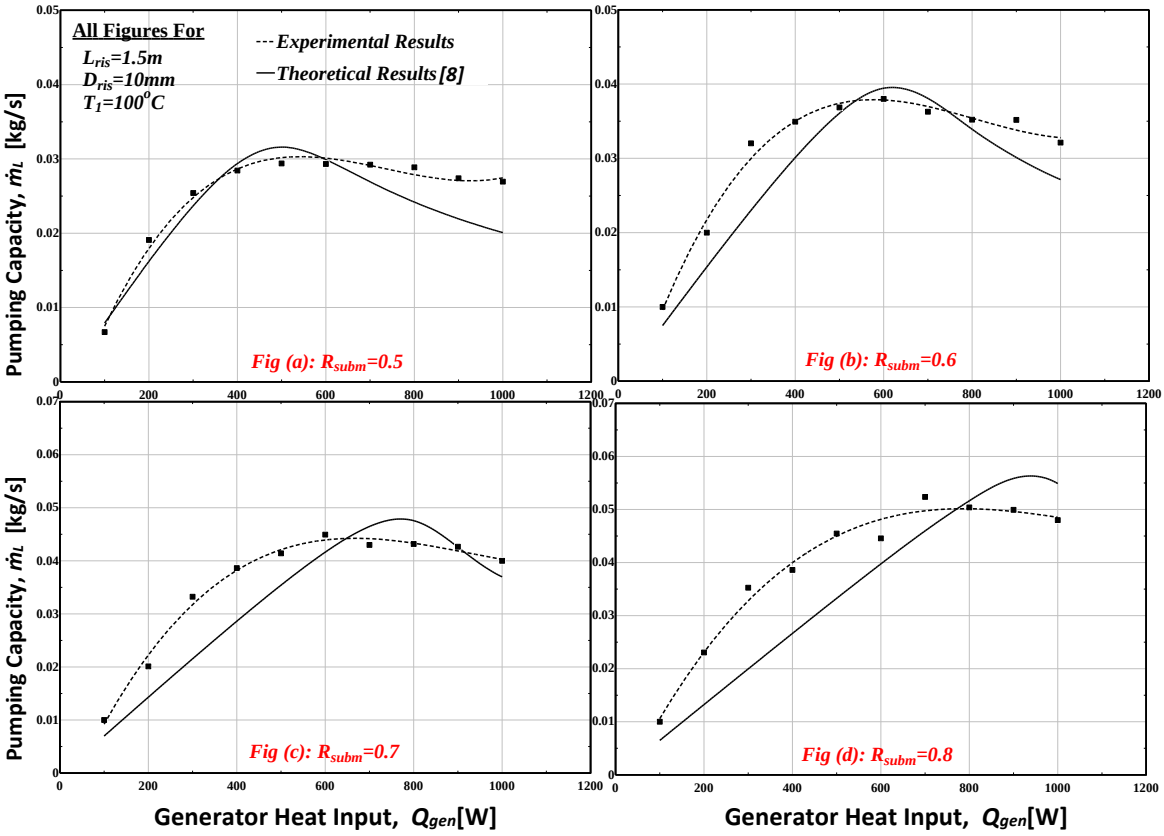

Fig.6 Variation of experimental and theoretical pumping capacity with generator heat input for riser diameter $D_{ris} = 10mm$ and input temperature of 100°C.

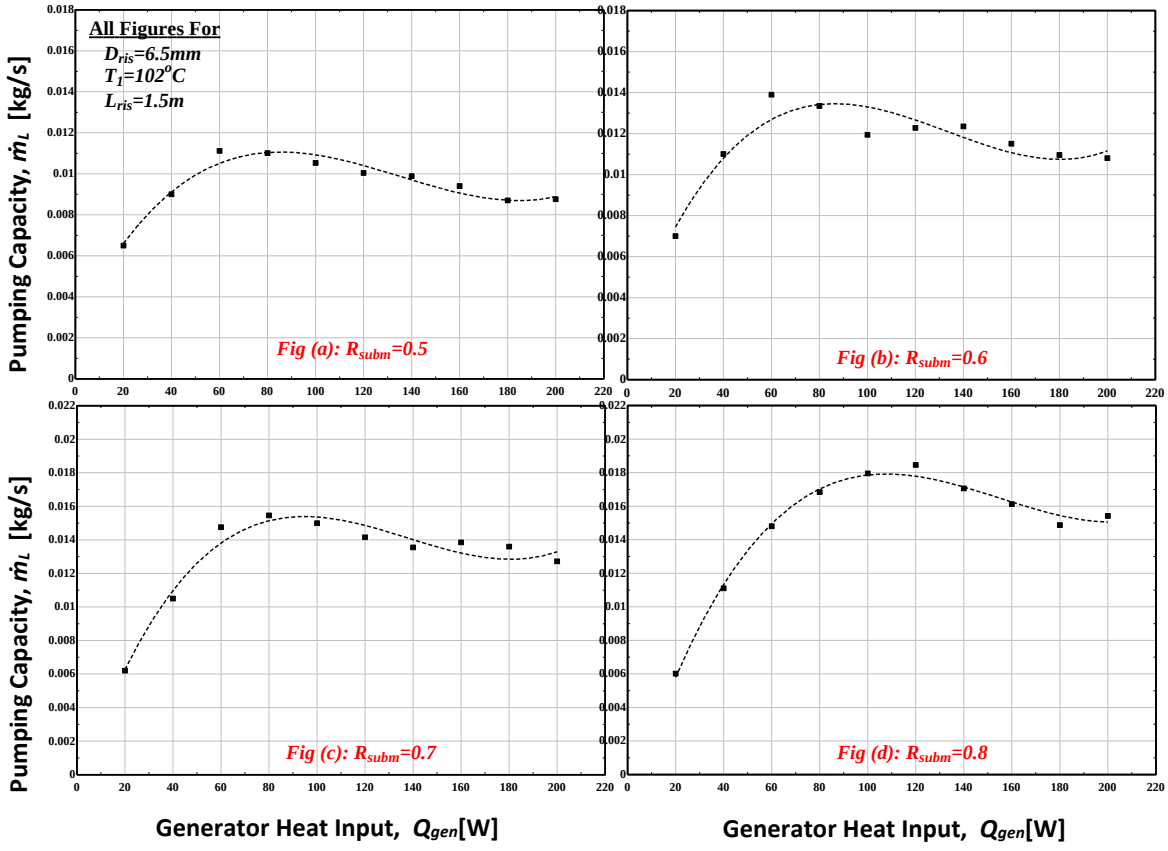

Fig.7 Variation of experimental pumping capacity with generator heat input for riser diameter $D_{ris} = 6.5mm$ and input temperature of 102°C.

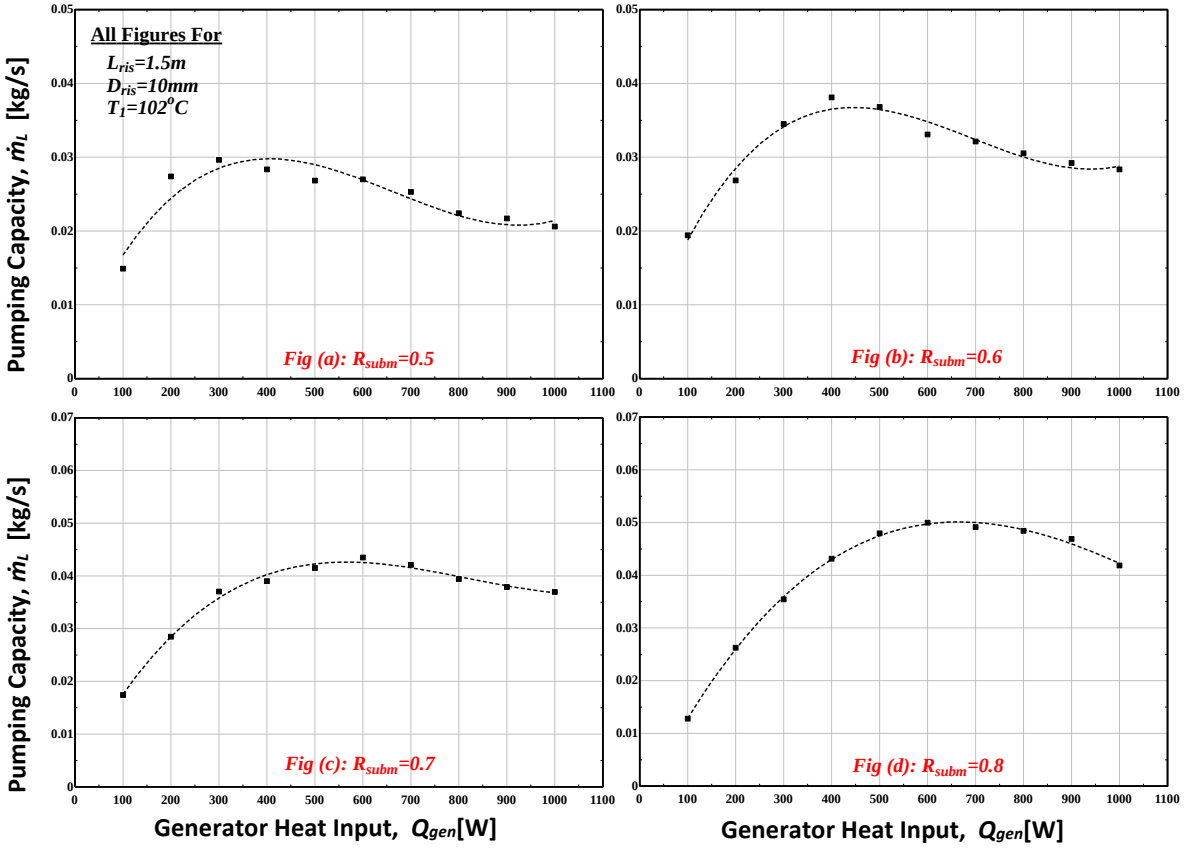

Fig.8 Variation of experimental pumping capacity with generator heat input for riser diameter $D_{ris} = 10mm$ and input temperature of 102°C.

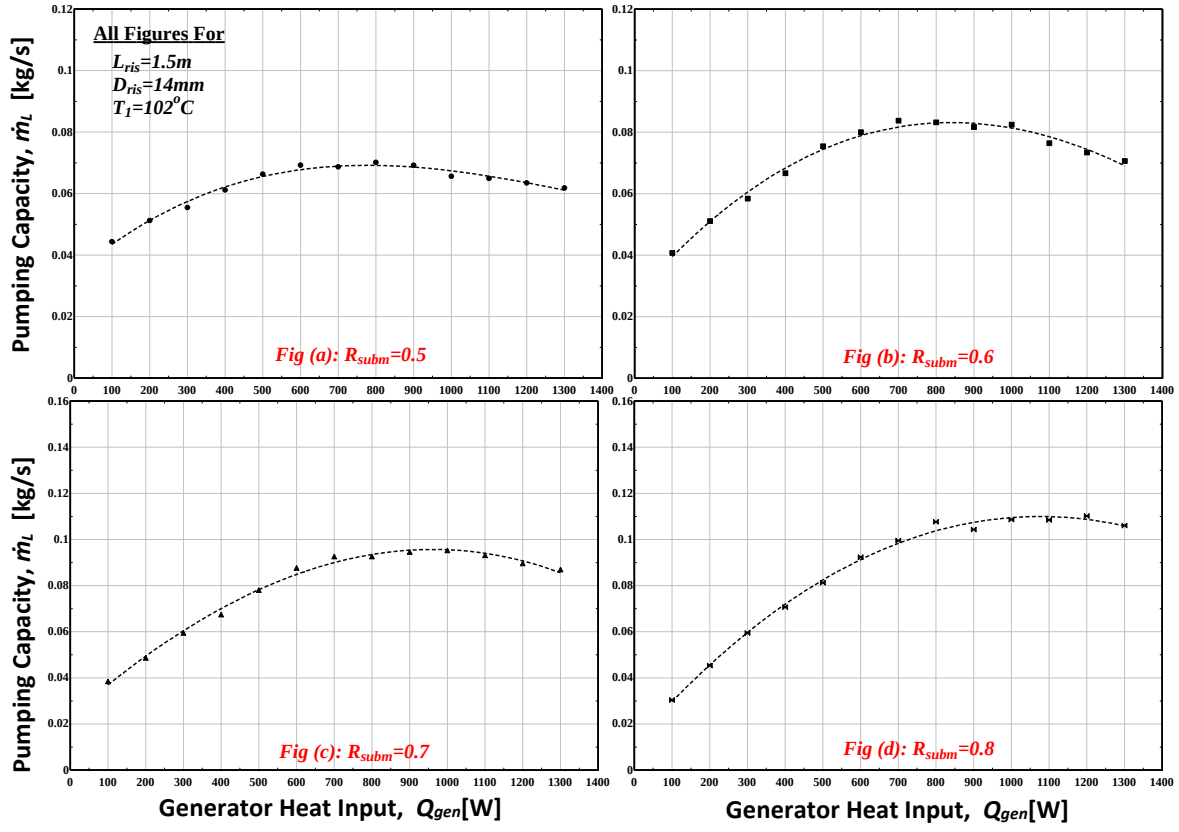

Fig.9 Variation of experimental pumping capacity with generator heat input for riser diametr $D_{ris} = 14mm$ and input temperature of 102°C.

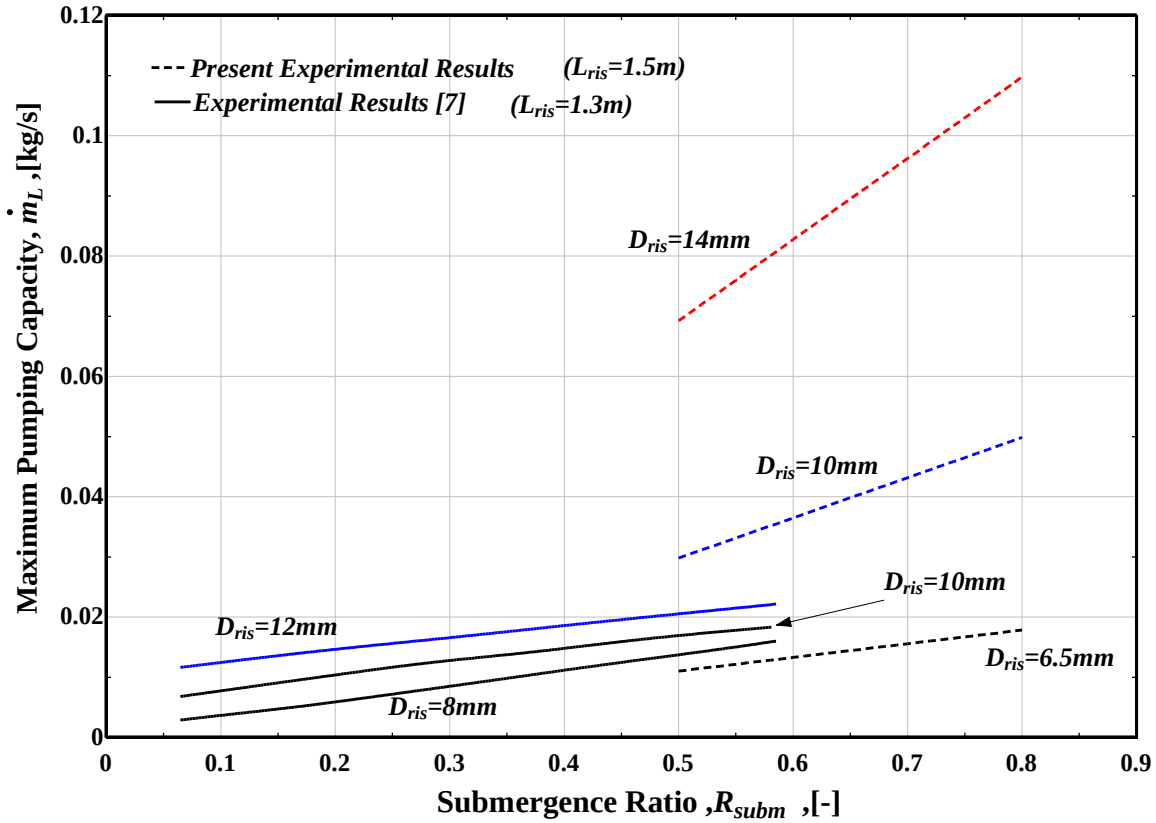

Fig.10 Comparison of experimental maximum pumping capacity with that obtained by [7].

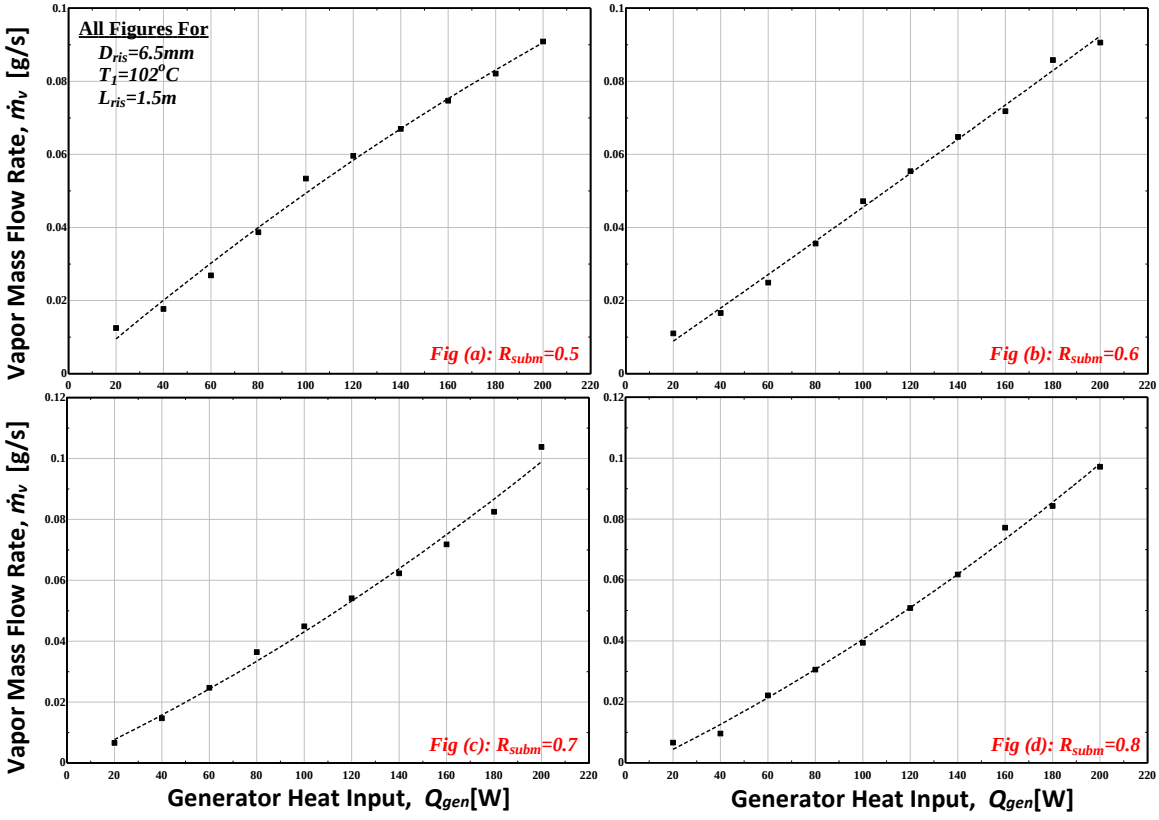

Fig. 11 Variation of experimental vapor mass flow with generator heat input for riser diameter $D_{ris} = 6.5mm$ and input temperature of 102ºC.

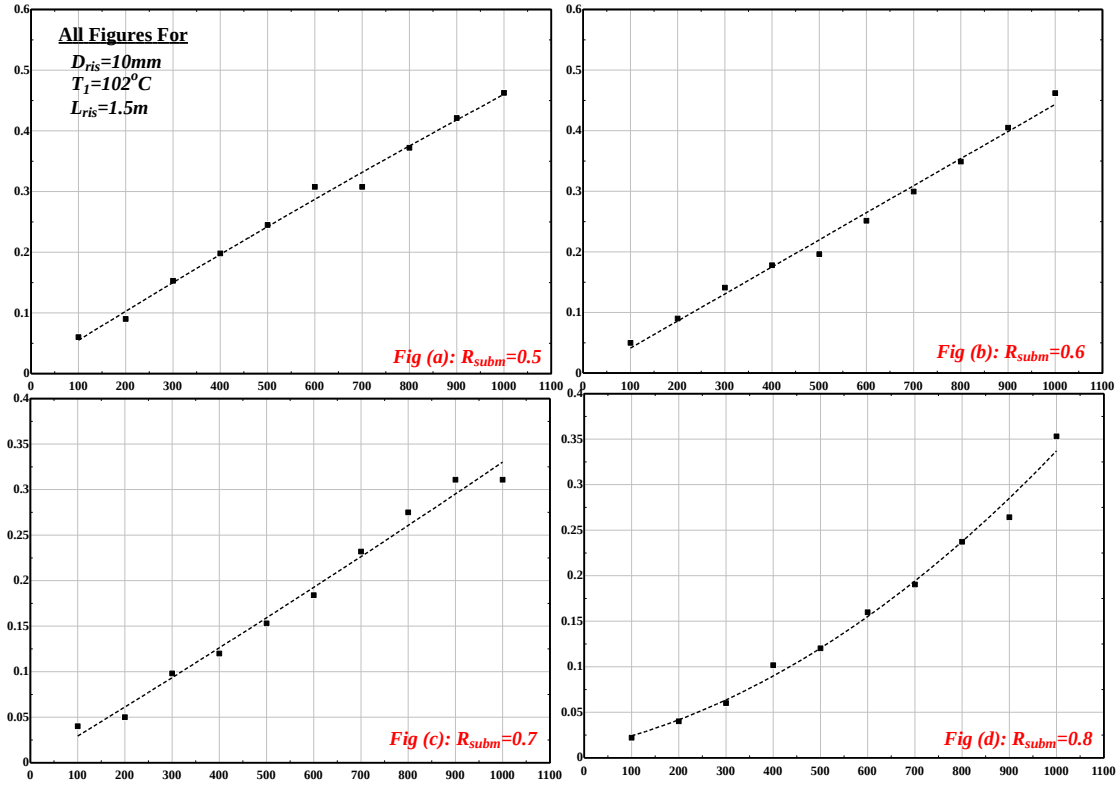

Fig.12 Variation of experimental vapor mass flow with generator heat input for riser diameter $D_{ris} = 10mm$ and input temperature of 102ºC.

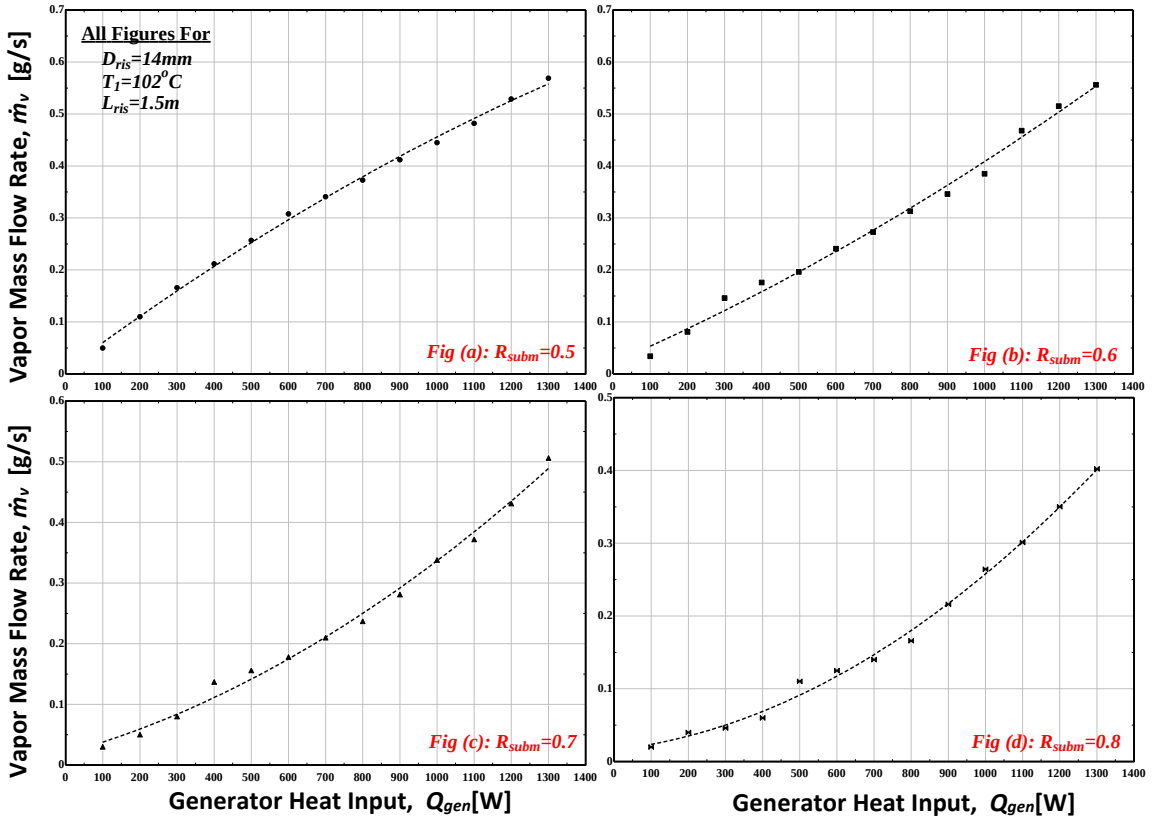

Fig.13 Variation of experimental vapor mass flow with generator heat input for riser diameter $D_{ris} = 14mm$ and input temperature of 102ºC.